https://dx.doi.org/10.1016/j.radonc.2023.109948

[Article Full Title]

Ultra-fast multi-parametric 4D-MRI image reconstruction for real-time applications using a Downsampling-Invariant Deformable Registration (D2R) model

[Short Title]

D2R Model for real-time 4D-MRI

[Author Names]

Haonan Xiao[1,2], Xinyang Han[1], Shaohua Zhi[1], Yat-Lam Wong[1], Chenyang Liu[1], Wen Li[1], Weiwei Liu[3], Weihu Wang[3], Yibao Zhang[3], Hao Wu[3], Ho-Fun Victor Lee[4], Lai-Yin Andy Cheung[4], Hing-Chiu Chang[5], Yen-Peng Liao[6], Jie Deng[6], Tian Li[1], Jing Cai[1]

[Author Institutions]

[1] Department of Health Technology and Informatics, The Hong Kong Polytechnic University, Hong Kong SAR, 999077, China

[2] Shandong Cancer Hospital and Institute, Shandong First Medical University and Shandong Academy of Medical Sciences

[3] Key Laboratory of Carcinogenesis and Translational Research (Ministry of Education/Beijing), Department of Radiation Oncology, Beijing Cancer Hospital & Institute, Peking University Cancer Hospital & Institute, Beijing, 100000, China

[4] Department of Clinical Oncology, The University of Hong Kong, Hong Kong SAR, 999077, China

[5] Department of Biomedical Engineering, The Chinese University of Hong Kong, Hong Kong SAR, 999077, China

[6] Department of Radiation Oncology's Division of Medical Physics & Engineering, University of Texas Southwestern Medical Center, Texas, 75390, USA

[Corresponding Author Name, Mailing and Email Address]

Jing Cai, corresponding author

jing.cai@polyu.edu.hk

Department of Health Technology and Informatics, The Hong Kong Polytechnic University, Hung Hom, Kowloon, Hong Kong

Tian Li, co-corresponding author

litian.li@polyu.edu.hk

Department of Health Technology and Informatics, The Hong Kong Polytechnic University, Hung Hom, Kowloon, Hong Kong

[Author Responsible for Statistical Analysis Name & Email Address]

Haonan Xiao

hao-nan.xiao@polyu.edu.hk

Department of Health Technology and Informatics, The Hong Kong Polytechnic University, Hung Hom, Kowloon, Hong Kong

[Funding Statement]

This research was partly supported by research grants of General Research Fund (GRF 15102219, GRF 15104822), the University Grants Committee, Health and Medical Research Fund (HMRF 06173276), the Health Bureau, Hong Kong Special Administrative Regions, and National Institutes of Health (NIH R01 CA226899), The United States of America.

[Data Availability Statement for this Work]

Research data are not available at this time.

[Conflict of Interest Statement for All Authors]

Dr. Jing Cai received research grants from General Research Fund (GRF 15102219), the University Grants Committee, Health and Medical Research Fund (HMRF 06173276), the Health Bureau, Hong Kong Special Administrative Regions, and National Institutes of Health (NIH R01 CA226899), The United States of America. Dr. Tian Li received research grant from General Research Fund (GRF 15104822), the University Grants Committee, Hong Kong Special Administrative Regions. Other authors have nothing to disclose.

Abstract

Background and purpose: Motion estimation from severely downsampled 4D-MRI is essential for real-time imaging and tumor tracking. This simulation study developed a novel deep learning model for simultaneous MR image reconstruction and motion estimation, named the Downsampling-Invariant Deformable Registration (D2R) model.

Materials and methods: Forty-three patients undergoing radiotherapy for liver tumors were recruited for model training and internal validation. Five prospective patients from another center were recruited for external validation. Patients received 4D-MRI scans and 3D MRI scans. The 4D-MRI was retrospectively down-sampled to simulate real-time acquisition. Motion estimation was performed using the proposed D2R model. The accuracy and robustness of the proposed D2R model and baseline methods, including Demons, Elastix, the parametric total variation (pTV) algorithm, and VoxelMorph, were compared. High-quality (HQ) 4D-MR images were also constructed using the D2R model for real-time imaging feasibility verification. The image quality and motion accuracy of the constructed HQ 4D-MRI were evaluated.

Results: The D2R model showed significantly superior and robust registration performance than all the baseline methods at downsampling factors up to 500. HQ T1-weighted and T2-weighted 4D-MR images were also successfully constructed with significantly improved image quality, sub-voxel level motion error, and real-time efficiency. External validation demonstrated the robustness and generalizability of the technique.

Conclusion: In this study, we developed a novel D2R model for deformation estimation

of downsampled 4D-MR images. HQ 4D-MR images were successfully constructed using the D2R model. This model may expand the clinical implementation of 4D-MRI for real-time motion management during liver cancer treatment.

Keywords: real-time, motion management, 4D-MRI, deformable image registration, deep learning

Highlights

- We proposed a deep learning registration model that is robust to downsampling artifacts.
- We used the deep learning model to reconstruct high-quality multi-parametric 4D-MRI from severely downsampled images.
- The model was validated by external prospective data.
- The reconstruction is promising to provide real-time efficiency.
- The proposed 4D-MRI method does not require special hardware or software and can be integrated into current clinical protocols.

1. Introduction

Magnetic resonance imaging (MRI) has shown great capabilities for image guidance during radiation treatment (RT) of abdominal cancer, mainly because of its superior soft-tissue contrast. Usually, a high-quality pre-beam scan is performed before each treatment to acquire essential information, including daily anatomical changes, after which real-time images may be acquired during treatment to reflect tumor motion in real time[1-4]. However, real-time imaging mainly relies on two-dimensional (2D) cine-MRI, which provides limited choices for image contrast (mostly T2/T1-weighted) and incomplete motion information in only a few planes.

Four-dimensional (4D)-MRI, which contains one more time dimension than regular three-dimensional (3D)-MRI, provides both versatile image contrasts and complete motion information in all three directions[5-7]. Current 4D-MRI methods are usually limited by insufficient temporal resolution for real-time image guidance. The total latency between a motion and a reaction should be less than 500 ms to achieve real-time tracking during RT[8], yet 2D or 3D acquisition-based 4D-MRI methods usually require several minutes for image acquisition to obtain sufficient data[9]. Some studies have shown the feasibility of generating 4D-MR images by deforming prior 3D MR images[10,11]; however, in the real-time scenario, the time required for these methods is unacceptable. Consequently, to fully utilize a prior high-quality multiparametric (Mp) 3D-MR image, it is of vital importance to obtain real-time 3D motion information in the entire field of view.

Current real-time motion estimation and 4D-MRI methods are mostly based on

motion modeling. For example, 3D deformation vector fields (DVFs) may be inferred from dynamic images, such as inferring 3D deformation vector fields (DVFs) from one-dimensional projections or 2D cine-MR images[12-15], external surrogates[16-19], or undersampled k-space data[20,21]. However, these model-based methods share similar limitations. First, they require individual modeling for each patient, and the motion information may be incomplete, as minor motion components may be ignored. Also, the models are usually not adaptive to patient anatomy changes throughout all the fractions. Second, they involve the use of extra devices, and the correlation between the external surrogates and organ deformations may be indirect. Third, patients are assumed to maintain a constant respiratory pattern, requiring extra efforts for breath coaching.

In recent years, deep learning models have been introduced for motion estimation, and these have successfully reduced the implementation time to milliseconds[22-24], thus meeting real-time requirements. Some studies have also demonstrated the feasibility of deformation estimation from extremely undersampled MR images using deep learning[25,26]. Although these methods have shown promising results, the deep learning models receive downsampled MR images directly, and downsampling artifacts may easily mislead the motion estimation.

In this study, we propose a deep learning model, the Downsampling-Invariant Deformable Registration (D2R) model, for simultaneous 4D-MRI reconstruction and motion estimation, and high-quality (HQ) T1-weighted (T1w) and T2-weighted (T2w) 4D-MR images construction. The D2R model includes a reconstruction branch and a registration branch. The former branch reconstructs images from downsampled 4D-

MRI using a densely connected convolutional neural network, while the latter branch receives the reconstructed images and predicts accurate deformations. The performance and robustness of the D2R model were compared with baseline iterative methods and deep learning models. The constructed HQ 4D-MR images were evaluated by tumor motion accuracy and image quality metrics.

2. Materials and methods

2.1 Patient data

The data used in this study was from two centers and both obtained the institutional review board approval. Forty-three patients were from Beijing Cancer Hospital (BJCH) with the approval number 2021YJZ05. These patients were used for model training and internal validation. Five patients were prospectively collected from University of Texas Southwestern Medical Center (UTSW) as external validation dataset with the approval number STU 082013-008. Detailed patient information is provided in supplementary **Appendix A**.

For BJCH patients, each of them received a 4D-MRI scan using a commercially available sequence. Hereafter, such scan is referred to as "low-quality (LQ) 4D-MRI." Thirty-one of them also received regular T1w (free-breathing) and T2w (gated) 3D MRI scans. The 3D scans were performed just prior to the 4D scans to avoid possible anatomical changes. Patients with low respiratory amplitude or severe motion artifacts were excluded from model training, but were included for HQ Mp 4D-MRI construction in later procedures. The remaining twenty-five patients used for five-fold

cross-validation. UTSW patients received 4D-MRI scans and T2w (gated) 3D MRI scans. They were not involved in model training and were only used for HQ 4D-MRI construction. The details of the MRI acquisition and pre-processing are provided in supplementary **Appendix A**.

2.2 Real-time 4D-MRI acquisition simulation

As recommended by the American Association of Physicists in Medicine (AAPM)[8], real-time tracking requires a total latency less than 500 ms and an imaging frequency greater than 3 Hz. To achieve this, the MRI acquisition time should be no longer than 300 ms to allow sufficient time for image reconstruction, HQ Mp 4D-MRI construction, and radiation beam repositioning. **Appendix B** shows a retrospective downsampling method using non-uniform fast Fourier transform[1] (NUFFT) to simulate such a real-time scenario and generate 4D-MR images of downsampling factor ($\mathcal{R}$) up to 1013.

2.3 D2R model

D2R model was trained to obtain DVFs between the high-quality pre-beam 3D MR images and the dynamic LQ 4D-MR images. Therefore, the fixed images (I_{fix}) in all image pairs were downsampled retrospectively using the method introduced above. The downsampled fixed image (I_{fix}^{down}) was considered as the new respiratory position during treatment, and the moving image (I_{mov}) was intended to match it.

Figure 1 shows the network architecture of the proposed D2R model. It consists

[1] Available at https://github.com/andyschwarzl/gpuNUFFT

of a reconstruction branch and a deformable registration branch. The heavily undersampled k-space and the simple image reconstruction with inverse NUFFT resulted in severe artifacts in I_{fix}^{down}, and the blurred image content and poorly defined organ boundaries may have misled registration. A reconstruction branch was, therefore, needed to improve the image quality. The reconstructed image, I_{fix}^{recon}, and the moving image, I_{mov}, were then fed to the deformable registration branch for DVF prediction. Details of the D2R model are provided in **Appendix C**.

2.4 HQ Mp 4D-MR image construction

A D2R model-based HQ Mp 4D-MRI construction framework was proposed to demonstrate its potential for real-time imaging. An overview of the framework is shown in **Figure 2**. The 4D-MRI frame at the closest respiratory phase as the prior 3D Mp MRI was selected as the "best-matched frame." Prior image-based 4D-MRI methods often suffer from inevitable mismatches between 3D- and 4D-MR images and inaccurate image registration due to differences in image contrast. Registration is even more challenging when the 4D-MR image is retrospectively downsampled. The rationale for introducing the "best-matched frame" instead of direct registration was the avoidance of possible mismatches. The 4D-MRI frame of the maximal cross-correlation with the corresponding 3D-MR image was selected and registered to the 3D-MRI using Elastix[2] to address residual anatomical differences. Each alignment between 4D and 3D MR images was manually checked before further process. The registration would

[2] Available at https://github.com/raacampbell/matlab_elastix

be completed prior to the treatments and would not delay the tracking efficiency. This frame was considered as a representation of the 3D Mp MR image and was registered to all frames of the downsampled 4D-MRI using the D2R model to obtain the DVFs during the entire respiratory cycle, or a 4D-DVF. The 4D-DVF was then applied to the 3D Mp MR images to construct HQ Mp 4D-MR images at the corresponding frames. All alignments were manually verified before HQ Mp 4D-MRI reconstruction.

2.5 Evaluation

Typical iterative and deep learning registration methods, including Demons[27], Elastix[28], the pTV algorithm[29], and VoxelMorph[30] were included as baseline methods for comparison, and the details are shown in supplementary **Appendix D**. Image similarity metrics, including the structure similarity index measure (SSIM), peak signal-to-noise ratio (PSNR), and mean squared error (MSE) were used for assessment and t-tests were performed to evaluate the significance of these quantitative metrics, with a threshold *p*-value of 0.05.

Region-of-interest (ROI) motion accuracy is an essential component of HQ Mp 4D-MRI. A region-matching-based program was developed in MATLAB (Version 9.11.0.1769968 [R2021b]; MathWorks Inc., Natick, MA, USA)[31] and the ROI motion trajectories were recorded in the superior–inferior (SI), anterior–posterior (AP), and medial–lateral (ML) directions. Images were interpolated before measurement to achieve a motion resolution of 0.33 mm.

Image quality improvement from the LQ 4D-MRI to the HQ Mp 4D-MRI was

quantified using several metrics. First, tumor contrast enhancement was quantified using the contrast-to-noise ratio (CNR). Second, overall image blurring was evaluated using a no-reference perceptual blur metric (PBM)[32]. Third, organ boundary sharpness was quantified using full-width-at-half-maximum (FWHM) value at the lung–liver edges[33]. For measurements involving manual contours, i.e., CNR and lung–liver edge FWHM measurements, the procedures were repeated three times, and the average value was reported to reduce randomness.

3. Results

Figure 3(a) plots the performance evaluation metrics of the D2R model versus the downsampling factor $\mathcal{R}$. The D2R model gave consistent image similarity at $\mathcal{R}$ values as high as 500 while the iterative methods were misled by downsampling artifacts and outputted twisted images. Specifically, as 100 radial spokes in k-space were used in subsequent HQ Mp 4D-MR image construction, a comparison of these methods at $\mathcal{R}$ = 253 (100 radial spokes) was performed, and the results are shown in **Figure 3(b)**. The D2R model showed significantly higher values than all the baseline methods for all similarity metrics ($p < 0.05$).

Figure 4 demonstrates two registration examples. The I_{fix}^{down} showed severe artifacts, and the results from iterative methods were all twisted because of their nature of aligning pixel intensities. Also, the image similarity metrics noticeably decreased to levels even lower than those without registration. In contrast, the two deep learning models outputs plausible results since they have seen the anatomical atlas during

training. The D2R model gave more accurate results compared to VoxelMorph thanks to the image quality enhancement of I_{fix}^{recon} from the reconstruction branch.

Figure 5(a) displays LQ, downsampled, and HQ Mp 4D-MR images of a patient in six frames, with the tumor position indicated by arrows. A video of the 4D-MR image of this patient was available in the supplementary material. The downsampled image had degraded quality, while the HQ T1w image had better-defined structures and higher tumor CNR of 7.7, compared to 1.9 in the LQ image. Compared to the LQ 4D-MR image, the PBM value in the HQ T1w images decreased from 0.700 to 0.427, and the FWHM value of the lung–liver edge decreased from 11.49 mm to 7.99 mm and from 9.81 mm to 9.26 mm in the cross-plane and in-plane directions, respectively. Tumor visibility was further improved in the HQ T2w 4D-MR image, which had the highest CNR of 14.4. The PBM value decreased to 0.395, and the FWHM value of the lung–liver edge decreased to 7.84 mm and 5.13 mm in the cross-plane and in-plane directions for the HQ T2w 4D-MR image. Motion was accurately reflected in the generated HQ Mp 4D-MR images, and the tracked motion trajectories was plotted in **Figure E.1** in supplementary **Appendix E**, where tumor motion matched with the LQ 4D-MR image, with a maximum error within 2 mm.

HQ Mp 4D-MR images were successfully obtained for the thirty-one patients from BJCH with both 4D-MRI and 3D MRI scans. The implementation time of the D2R model was 4.5 ± 0.6 ms on the same workstation as training. The ROI motion amplitude was measured for all patients, and statistical analysis of the mean motion error was presented in **Figure 5(b)** as box plots. The mean relative ROI motion errors of HQ Mp

4D-MR images were smaller than the voxel size of the LQ 4D-MRI. HQ Mp 4D-MR images exhibited significant improvement ($p < 0.001$) over LQ 4D-MR images in image quality metrics, including PBM, lung-liver edge sharpness, and tumor CNR, except the tumor CNR of HQ T1w 4D-MR images. Supplementary **Appendix F** provides further details of the results.

The LQ 4D-MR, downsampled 4D-MR, and HQ T2w 4D-MR images of an example patient in the external validation dataset are shown in **Figure 6(a)**. The image quality shows similar improvements as it is in the internal validation. The tumor motion trajectory of this patient was plotted in **Figure E.2** in supplementary **Appendix E**, where the HQ T2w 4D-MR images matched well with the LQ 4D-MR images. **Figure 6(b)** shows the quantitative image quality metric improvement from the LQ 4D-MR images (left) to HQ T2w 4D-MR images (right), in which each line represents a patient The HQ T2w 4D-MR images over all show well matched motion and improved image quality.

4. Discussion

To our knowledge, the D2R model is the first deep learning model to integrate downsampled 4D-MRI reconstruction and motion estimation, showing superiority and robustness in downsampled 4D-MR images with R up to 500. The HQ Mp 4D-MR images constructed using the D2R model showed significantly improved image quality and yielded accurate tumor motion trajectories. The whole construction process was

less than 500 ms, and the simulated image acquisition frequency was greater than 3 Hz, promising real-time tumor tracking with 4D-MRI.

Iterative methods, including Demons, Elastix, and the pTV algorithm, outputted twisted images when executing downsampled 4D-MRI registration due to pixel intensity-based optimization. In contrast, deep learning models learned the overall anatomical structures during training and were able to predict accurate DVFs. Although the downsampled fixed images contained many artifacts, the moving image in training was of higher quality and from which D2R model views well-defined organ boundaries, aiding accurate deformation estimation. Besides, its reconstruction branch provides enhanced fixed images to its registration branch, also helping its superior performance.

Deep learning-based 4D-MRI reconstruction has been a hot topic in recent years and many interesting studies have been proposed. For example, Freedman et al. developed a model named Dracula for rapid 4D-MRI reconstruction[34], and Küstner et al. introduced additional motion correction into the reconstruction model for better performance[35]. However, many of these studies have primarily focused on improving image quality, rather than optimizing workflows for real-time applications. Freedman et al. spent about 28 seconds to reconstruct the images for one patient and Küstner et al. spent 90 seconds in image acquisition and another 35 seconds in image reconstruction. By contrast, our study simulated an acquisition time of 0.3 second and reconstructed the images in milli-seconds, aiming for real-time target tracking during treatment.

The D2R model has several advantages over current real-time motion estimation or

4D-MRI methods. First, this method does not require patient-specific modeling and may therefore be universal, saving time and computational resources in clinical implementation. Second, this method does not assume motion similarity between the training scans and those acquired during treatment, reducing the need for patient breathing coaching. Third, this method provides images, rather than just DVFs, for visualizing patient motion and serving as a quality assurance indicator if exceptional motion occurs. Finally, this method may provide multiple MRI contrasts simultaneously, benefiting other online applications such as segmentation.

The motivation for constructing HQ Mp 4D-MR images was to demonstrate the feasibility of the D2R model for real-time imaging. The imaging acquisition theoretically takes less than 300 ms per frame, which meets the imaging frequency requirement. GPU-based NUFFT reconstruction takes approximately 50 ms per volume, D2R model implementation takes 4.5 ± 0.6 ms per frame, and modern MLC tracking takes approximately 80 ms to reposition the radiation beam[36]. The total latency may be as short as 500 ms and the imaging frequency is greater than 3 Hz, satisfying the real-time requirement[8] and promising the application of 4D-MRI in real-time tumor tracking. A noteworthy point is that the data processing may need a powerful workstation instead of the computers associated with the MR scanners, and the data loading and transferring can take extra time in the real clinic. The average ROI tracking error in the HQ Mp 4D-MRI was highest in the SI direction, at 1.18 ± 1.20 mm. This may be acceptable for liver stereotactic body RT, as a margin of 1.5 mm is usually applied during planning[37].

The robustness and generalizability of our HQ 4D-MRI technique has been

validated on the prospective external dataset from UTSW. Despite the differences on the MR scanner, imaging sequence, and clinical protocols, the technique successfully constructed HQ 4D-MR images with improved image quality and well-matched tumor motion trajectories. These results not only reinforce the robustness and generalizability of our method but also provide tangible evidence of its applicability in the clinic.

Despite the promising results, this study has some limitations. First, the downsampling was retrospective and simulated. The upper limit of the downsampled 4D-MR image was the LQ 4D-MR image instead of the actual patient. Also, the simulation simplifies the processing of the k-space data, such as data transferring and coil sensitivity compensation. Although we expect that our method will perform better on actual patients, extra delays could be introduced into the reconstruction because of the k-space data processing. We will acquire k-space data and evaluate the technique in real clinical settings in our future studies. Second, the downsampled images would be of better quality if using deep-learning-based reconstruction or super-resolution methods[38,39] and potentially improve the deformation estimation accuracy. Lastly, the images collected were not single-phase, especially the respiratory-averaged T1w images from BJCH. Even in the gated images, the tumor size can be larger than its actual size and the enlarged volume could be its transverse area times up to 20% of the patient's breathing amplitude in the SI direction, as the gating was set at the last 20% amplitude of the inhalation process. We will prospectively design a more appropriate protocol for acquisition to balance the image quality and efficiency and provide better images for HQ 4D-MRI reconstruction in later studies.

5. Conclusions

In this study, we developed a novel D2R model for deformation estimation of retrospectively downsampled 4D-MR images. The performance of the model was consistent at downsampling factors up to 500. HQ Mp 4D-MR images, including T1w and T2w images, were successfully constructed using the D2R model with significantly improved image quality, sub-voxel-level tumor motion trajectories, and real-time efficiency. This new method may expand the clinical implementation of 4D-MRI for real-time motion management during RT for liver cancer.

Reference

1. Raaymakers BW, Jürgenliemk-Schulz IM, Bol GH, et al. First patients treated with a 1.5 T MRI-Linac: clinical proof of concept of a high-precision, high-field MRI guided radiotherapy treatment. *Phys Med Biol*. Nov 14 2017;62(23):L41-l50. doi:10.1088/1361-6560/aa9517

2. van de Lindt TN, Fast MF, van den Wollenberg W, et al. Validation of a 4D-MRI guided liver stereotactic body radiation therapy strategy for implementation on the MR-linac. *Phys Med Biol*. 2021;66(10):105010.

3. Ristau J, Horner-Rieber J, Buchele C, et al. Stereotactic MRI-guided radiation therapy for localized prostate cancer (SMILE): a prospective, multicentric phase-II-trial. *Radiat Oncol*. Apr 15 2022;17(1):75. doi:10.1186/s13014-022-02047-w

4. Hal WA, Straza MW, Chen X, et al. Initial clinical experience of Stereotactic Body Radiation Therapy (SBRT) for liver metastases, primary liver malignancy, and pancreatic cancer with 4D-MRI based online adaptation and real-time MRI monitoring using a 1.5 Tesla MR-Linac. *PLoS One*. 2020;15(8):e0236570. doi:https://doi.org/10.1371/journal.pone.0242146

5. Liu Y, Yin FF, Czito BG, Bashir MR, Cai J. T2-weighted four dimensional magnetic resonance imaging with result-driven phase sorting. *Med Phys*. 2015;42(8):4460-4471. doi:10.1118/1.4923168

6. Liu Y, Zhong X, Czito BG, et al. Four-dimensional diffusion-weighted MR imaging (4D-DWI): a feasibility study. *Med Phys*. 2017;44(2):397-406. doi:10.1002/mp.12037

7. Cai J, Chang Z, Wang Z, Paul Segars W, Yin FF. Four-dimensional magnetic resonance imaging (4D-MRI) using image-based respiratory surrogate: a feasibility study. *Med Phys*. Dec

2011;38(12):6384-94. doi:10.1118/1.3658737

8. Keall PJ, Sawant A, Berbeco RI, et al. AAPM Task Group 264: The safe clinical implementation of MLC tracking in radiotherapy. 10.1002/mp.14625. *Med Phys*. 2021/05/01 2021;48(5):e44-e64. doi:10.1002/mp.14625

9. Stemkens B, Paulson ES, Tijssen RH. Nuts and bolts of 4D-MRI for radiotherapy. *Phys Med Biol*. 2018;63(21):21TR01. doi:10.1088/1361-6560/aae56d

10. Li G, Wei J, Kadbi M, et al. Novel Super-Resolution Approach to Time-Resolved Volumetric 4-Dimensional Magnetic Resonance Imaging With High Spatiotemporal Resolution for Multi-Breathing Cycle Motion Assessment. *Int J Radiat Oncol Biol Phys*. 2017;98(2):454-462. doi:10.1016/j.ijrobp.2017.02.016

11. Li G, Sun A, Nie X, et al. Introduction of a pseudo demons force to enhance deformation range for robust reconstruction of super-resolution time-resolved 4DMRI. *Med Phys*. Nov 2018;45(11):5197-5207. doi:10.1002/mp.13179

12. Feng L, Tyagi N, Otazo R. MRSIGMA: Magnetic Resonance SIGnature MAtching for real-time volumetric imaging. *Magn Reson Med*. Sep 2020;84(3):1280-1292. doi:10.1002/mrm.28200

13. Harris W, Ren L, Cai J, Zhang Y, Chang Z, Yin F-F. A technique for generating volumetric cine-magnetic resonance imaging. *International Journal of Radiation Oncology*Biology*Physics*. 2016/06/01/ 2016;95(2):844-853. doi:10.1016/j.ijrobp.2016.02.011

14. Harris W, Yin F-F, Cai J, Ren L. Volumetric cine magnetic resonance imaging (VC-MRI) using motion modeling, free-form deformation and multi-slice undersampled 2D cine MRI

reconstructed with spatio-temporal low-rank decomposition. *Quant Imaging Med Surg*. 2020;10(2):432-450. doi:10.21037/qims.2019.12.10

15. Harris W, Yin FF, Wang C, Zhang Y, Cai J, Ren L. Accelerating volumetric cine MRI (VC-MRI) using undersampling for real-time 3D target localization/tracking in radiation therapy: a feasibility study. *Phys Med Biol*. Dec 14 2017;63(1):01nt01. doi:10.1088/1361-6560/aa9746

16. McClelland JR, Modat M, Arridge S, et al. A generalized framework unifying image registration and respiratory motion models and incorporating image reconstruction, for partial image data or full images. *Phys Med Biol*. Jun 7 2017;62(11):4273-4292. doi:10.1088/1361-6560/aa6070

17. Li R, Lewis JH, Berbeco RI, Xing L. Real-time tumor motion estimation using respiratory surrogate via memory-based learning. *Phys Med Biol*. Aug 7 2012;57(15):4771-86. doi:10.1088/0031-9155/57/15/4771

18. Andreychenko A, Raaijmakers AJ, Sbrizzi A, et al. Thermal noise variance of a receive radiofrequency coil as a respiratory motion sensor. *Magn Reson Med*. Jan 2017;77(1):221-228. doi:10.1002/mrm.26108

19. Odille F, Cîndea N, Mandry D, Pasquier C, Vuissoz PA, Felblinger J. Generalized MRI reconstruction including elastic physiological motion and coil sensitivity encoding. *Magn Reson Med*. Jun 2008;59(6):1401-11. doi:10.1002/mrm.21520

20. Huttinga NRF, van den Berg CAT, Luijten PR, Sbrizzi A. MR-MOTUS: model-based non-rigid motion estimation for MR-guided radiotherapy using a reference image and minimal k-space data. *Phys Med Biol*. Jan 10 2020;65(1):015004. doi:10.1088/1361-6560/ab554a

21. Huttinga NRF, Bruijnen T, Van Den Berg CAT, Sbrizzi A. Real-Time Non-Rigid 3D

Respiratory Motion Estimation for MR-Guided Radiotherapy Using MR-MOTUS. *IEEE Trans Med Imaging*. Feb 2022;41(2):332-346. doi:10.1109/tmi.2021.3112818

22. Fu Y, Lei Y, Wang T, Curran WJ, Liu T, Yang X. Deep learning in medical image registration: a review. *Phys Med Biol*. Oct 22 2020;65(20):20TR01. doi:10.1088/1361-6560/ab843e

23. Xiao H, Teng X, Liu C, et al. A review of deep learning-based three-dimensional medical image registration methods. *Quant Imaging Med Surg*. Dec 2021;11(12):4895-4916. doi:10.21037/qims-21-175

24. Li C, Li W, Liu C, Zheng H, Cai J, Wang S. Artificial intelligence in multiparametric magnetic resonance imaging: A review. *Med Phys*. Oct 2022;49(10):e1024-e1054. doi:10.1002/mp.15936

25. Terpstra ML, Maspero M, Bruijnen T, Verhoeff JJC, Lagendijk JJW, van den Berg CAT. Real-time 3D motion estimation from undersampled MRI using multi-resolution neural networks. *Med Phys*. 2021;48(11):6597-6613. doi:10.1002/mp.15217

26. Terpstra ML, Maspero M, d'Agata F, et al. Deep learning-based image reconstruction and motion estimation from undersampled radial k-space for real-time MRI-guided radiotherapy. *Phys Med Biol*. Aug 7 2020;65(15):155015. doi:10.1088/1361-6560/ab9358

27. Thirion JP. Image matching as a diffusion process: an analogy with Maxwell's demons. *Med Image Anal*. Sep 1998;2(3):243-60. doi:10.1016/s1361-8415(98)80022-4

28. Klein S, Staring M, Murphy K, Viergever MA, Pluim JP. Elastix: a toolbox for intensity-based medical image registration. *IEEE Trans Med Imaging*. Jan 2009;29(1):196-205. doi:10.1109/TMI.2009.2035616

29. Vishnevskiy V, Gass T, Szekely G, Tanner C, Goksel O. Isotropic total variation regularization of displacements in parametric image registration. *IEEE Trans Med Imaging*. Feb 2016;36(2):385-395. doi:10.1109/TMI.2016.2610583

30. Balakrishnan G, Zhao A, Sabuncu MR, Guttag J, Dalca AV. VoxelMorph: a learning framework for deformable medical image registration. *IEEE Trans Med Imaging*. Feb 4 2019;doi:10.1109/TMI.2019.2897538

31. Xiao H, Ni R, Zhi S, et al. A dual-supervised deformation estimation model (DDEM) for constructing ultra-quality 4D-MRI based on a commercial low-quality 4D-MRI for liver cancer radiation therapy. *Med Phys*. May 2022;49(5):3159-3170. doi:10.1002/mp.15542

32. Crete F, Dolmiere T, Ladret P, Nicolas M. The blur effect: perception and estimation with a new no-reference perceptual blur metric. International Society for Optics and Photonics; 2007:64920I.

33. Ahmad R, Ding Y, Simonetti OP. Edge sharpness assessment by parametric modeling: application to magnetic resonance imaging. *Concepts Magn Reson Part A Bridg Educ Res*. May 1 2015;44(3):138-149. doi:10.1002/cmr.a.21339

34. Freedman JN, Gurney-Champion OJ, Nill S, et al. Rapid 4D-MRI reconstruction using a deep radial convolutional neural network: Dracula. *Radiother Oncol*. 2021/06/01/ 2021;159:209-217. doi:https://doi.org/10.1016/j.radonc.2021.03.034

35. Küstner T, Pan J, Gilliam C, et al. Self-Supervised Motion-Corrected Image Reconstruction Network for 4D Magnetic Resonance Imaging of the Body Trunk. *APSIPA Transactions on Signal and Information Processing*. 2022;11(1)doi:10.1561/116.00000039

36. Ng JA, Booth JT, O'Brien RT, et al. Quality assurance for the clinical implementation of

kilovoltage intrafraction monitoring for prostate cancer VMAT. *Med Phys*. Nov 2014;41(11):111712. doi:10.1118/1.4898119

37. Benedict SH, Yenice KM, Followill D, et al. Stereotactic body radiation therapy: the report of AAPM Task Group 101. *Med Phys*. Aug 2010;37(8):4078-101. doi:10.1118/1.3438081

38. Wang S, Xiao T, Liu Q, Zheng H. Deep learning for fast MR imaging: A review for learning reconstruction from incomplete k-space data. *Biomed Signal Process Control*. 2021/07/01/ 2021;68:102579. doi:10.1016/j.bspc.2021.102579

39. Huang B, Xiao H, Liu W, et al. MRI super-resolution via realistic downsampling with adversarial learning. *Phys Med Biol*. Oct 5 2021;66(20)doi:10.1088/1361-6560/ac232e

Figure captions

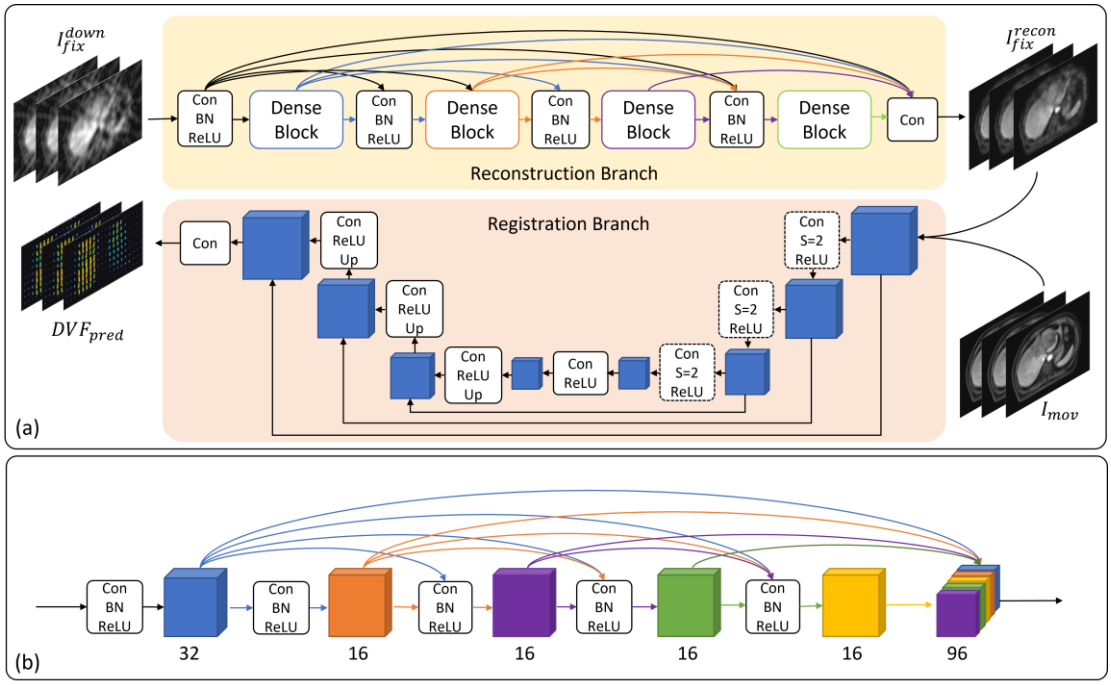

Figure 1: Network architecture of (a) the proposed D2R model and (b) the dense block.

Con: convolutional layer

BN: batch normalization layer; DVF_{pred}*: predicted DVF;* I_{fix}^{down}*: downsampled fixed image;* I_{fix}^{recon}*: reconstructed fixed image;* I_{mov}*: moving image; ReLU: rectified linear unit activation layer; Up: upsampling layer.*

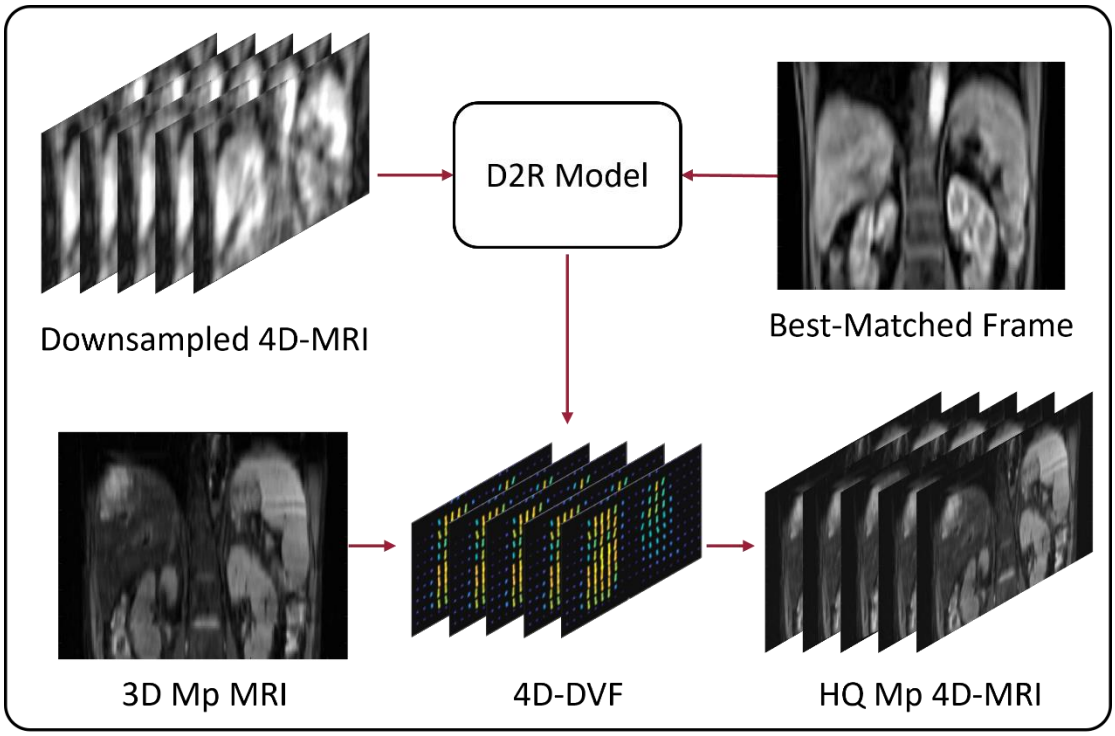

Figure 2: The HQ Mp 4D-MRI construction framework using the D2R model.

3D: three-dimensional; 4D: four-dimensional; D2R: downsampling-invariant deformable registration; DVF: displacement vector field; Mp: multiparametric; MRI: magnetic resonance imaging; HQ: high-quality.

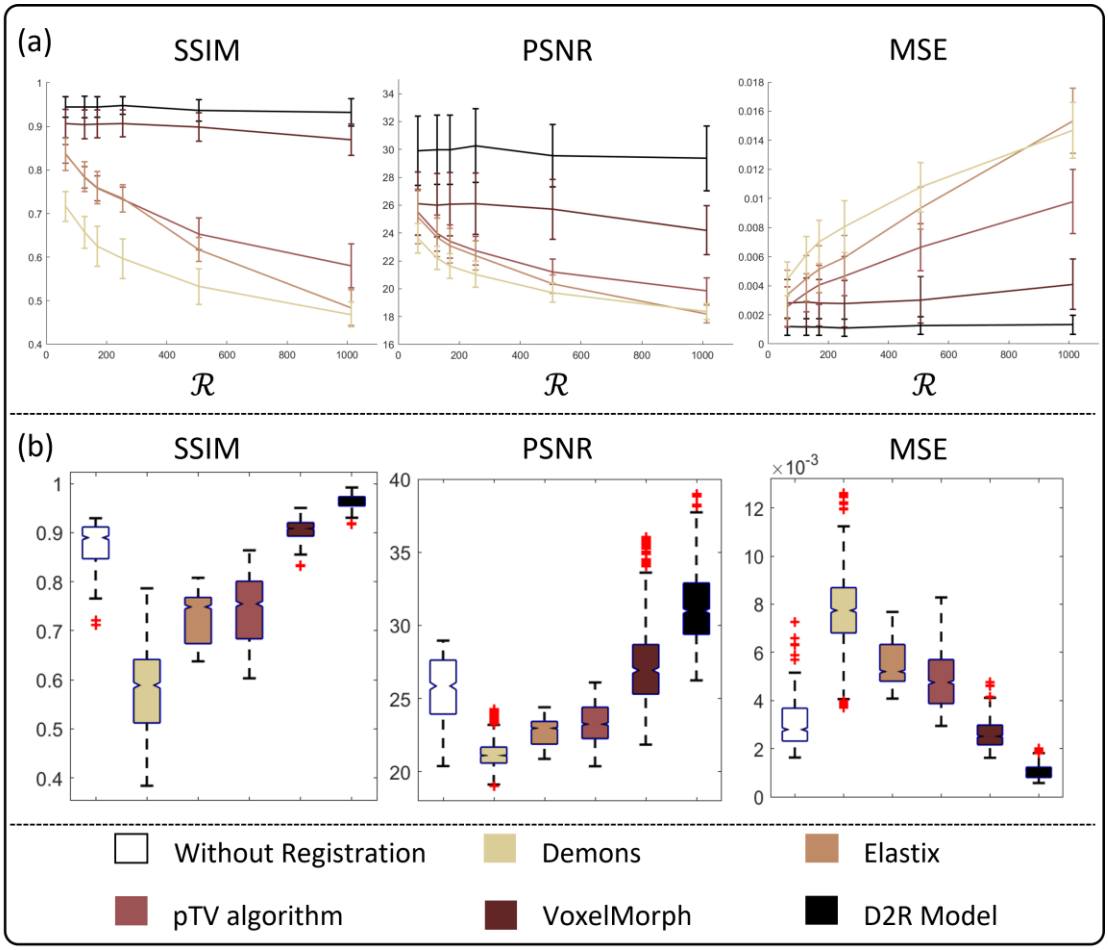

Figure 3: Registration performance of all tested methods. (a) Evaluation metrics versus the downsampling factor, $\mathcal{R}$. (b) Comparison of registration results at downsampling factor $\mathcal{R} = 253$ (100 radial spokes).

D2R: downsampling-invariant deformable registration; DVF: displacement vector field; MSE: mean squared error; PSNR: peak signal-to-noise ratio; pTV: parametric total variation; SSIM: structure similarity index measure.

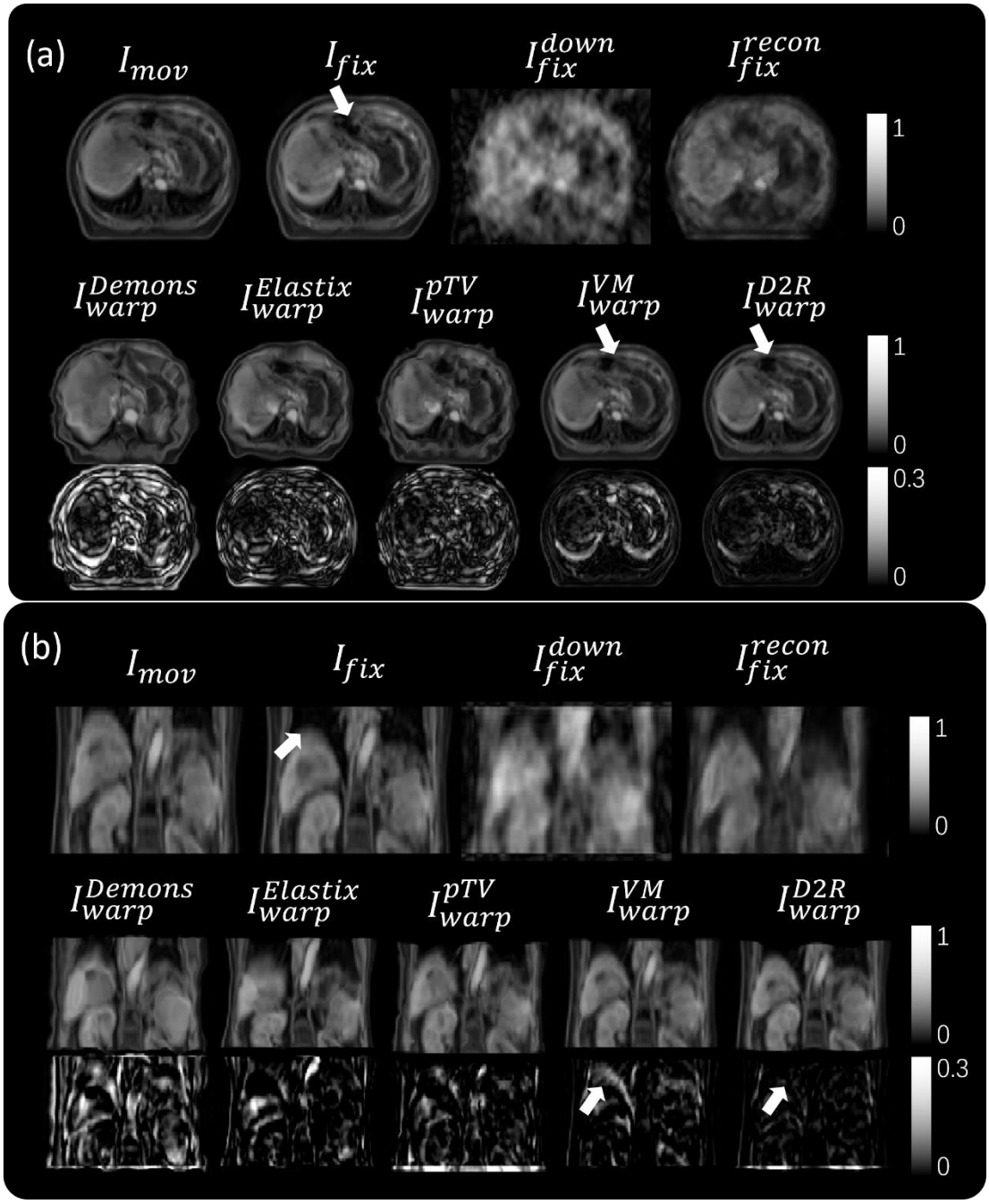

Figure 4: Examples of inputs (first row), registration results (second row), and difference map (third row) in the (a) axial view and (b) coronal view. White arrows indicate the superior accuracy of the D2R model over VoxelMorph.

I_{fix}: fixed image; I_{fix}^{down}: downsampled fixed image; I_{fix}^{recon}: reconstructed fixed image; I_{mov}: moving image; I_{warp}^{Demons}: warped image from Demons; $I_{warp}^{Elastix}$: warped image

from Elastix; I_{warp}^{pTV}*: warped image from pTV algorithm;* I_{warp}^{VM}*: warped image from Voxelmorph;* I_{warp}^{D2R}*: warped image from D2R model.*

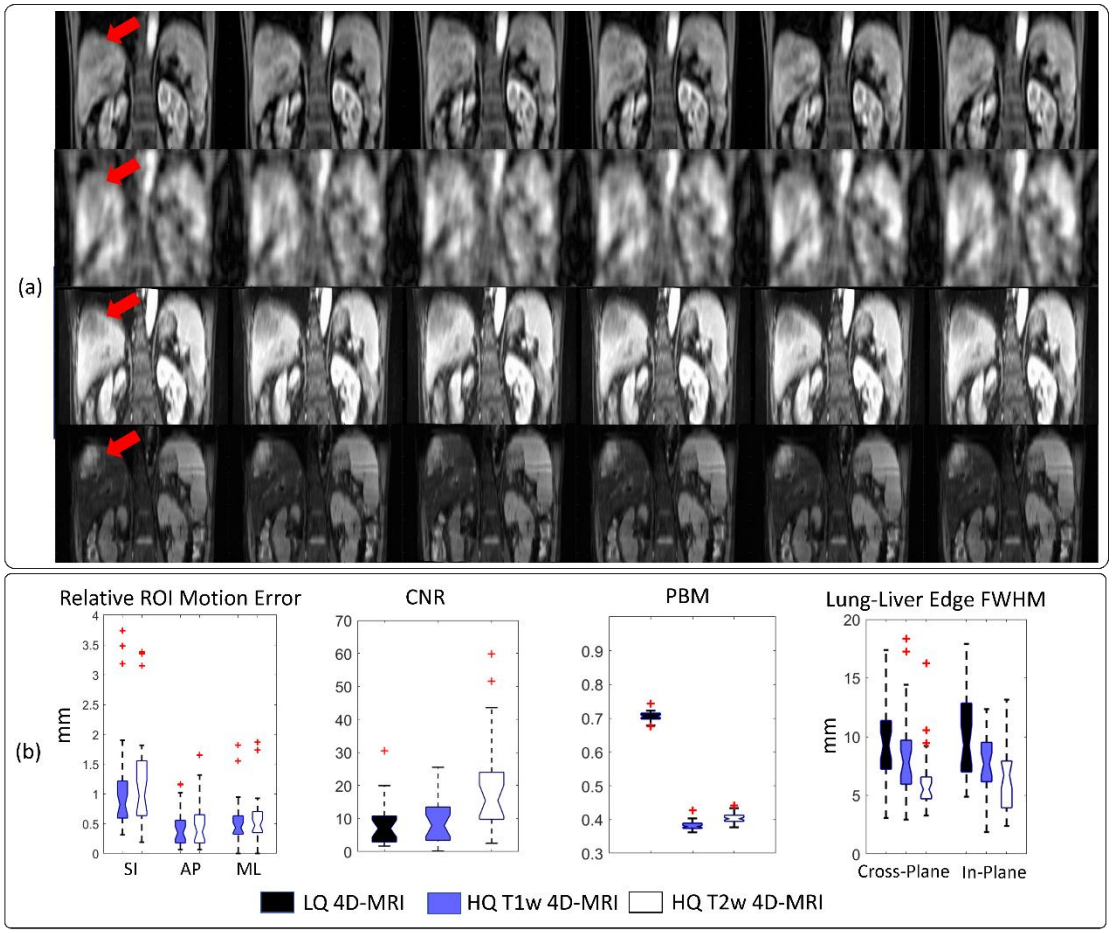

Figure 5: (a) (From top to bottom) The LQ 4D-MR image, downsampled 4D-MR image, HQ T1w 4D-MR image, and HQ T2w 4D-MR image of an example patient in the coronal view. Arrows indicate the tumor in the first frame. The images represent 3D volumes, but only 2D slices are shown for demonstration. (b) The relative ROI motion error (N = 31) in HQ Mp 4D-MR images, CNR (N = 22), PBM (N = 31), and lung–liver edge sharpness (N = 31) of different 4D-MR images.

4D-MRI: four-dimensional magnetic resonance imaging; AP: anterior–posterior; CNR: contrast-to-noise ratio; FWHM: full-width at half-maximum; ML: medial–lateral; PBM: perceptual blur metric; ROI: region-of-interest; SI: superior–inferior; T1w: T1-

weighted; T2w: T2-weighted; HQ: high-quality.

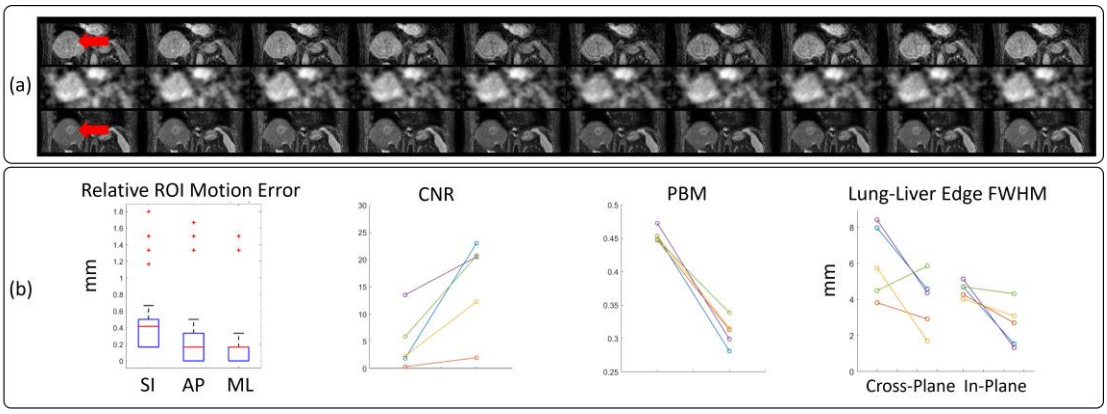

Figure 6: (a) (From top to bottom) The LQ 4D-MR image, downsampled 4D-MR image, and HQ T2w (SPIR) 4D-MR image of an example patient from the external dataset in the coronal view. Arrows indicate the tumor in the first frame. The images represent 3D volumes, but only 2D slices are shown for demonstration. (b) The relative ROI motion error (N = 5) in HQ T2w (SPIR) 4D-MRI, and image quality metrics (N = 5) of different 4D-MR images. Each line represents a patient, and it shows the image quality changes from the LQ 4D-MR images (left) to the HQ 4D-MR images (right).

4D-MRI: four-dimensional magnetic resonance imaging; AP: anterior–posterior; CNR: contrast-to-noise ratio; FWHM: full-width at half-maximum; ML: medial–lateral; PBM: perceptual blur metric; ROI: region-of-interest; SI: superior–inferior; T2w: T2-weighted; SPIR: Spectral Pre-saturation with Inversion Recovery; HQ: high-quality.